

Polarizations of J/ψ and $\psi(2S)$ Mesons Produced in $p\bar{p}$ Collisions at $\sqrt{s} = 1.96$ TeV

A. Abulencia,²⁴ J. Adelman,¹³ T. Affolder,¹⁰ T. Akimoto,⁵⁵ M. G. Albrow,¹⁷ S. Amerio,⁴³ D. Amidei,³⁵ A. Anastassov,⁵² K. Anikeev,¹⁷ A. Annovi,¹⁹ J. Antos,¹⁴ M. Aoki,⁵⁵ G. Apollinari,¹⁷ T. Arisawa,⁵⁷ A. Artikov,¹⁵ W. Ashmanskas,¹⁷ A. Attal,¹³ A. Aurisano,⁴² F. Azfar,⁴² P. Azzi-Bacchetta,⁴³ P. Azzurri,⁴⁶ N. Bacchetta,⁴³ W. Badgett,¹⁷ A. Barbaro-Galtieri,²⁹ V. E. Barnes,⁴⁸ B. A. Barnett,²⁵ S. Baroiant,⁷ V. Bartsch,³¹ G. Bauer,³³ P.-H. Beauchemin,³⁴ F. Bedeschi,⁴⁶ S. Behari,²⁵ G. Bellettini,⁴⁶ J. Bellinger,⁵⁹ A. Belloni,³³ D. Benjamin,¹⁶ A. Beretvas,¹⁷ J. Beringer,²⁹ T. Berry,³⁰ A. Bhatti,⁵⁰ M. Binkley,¹⁷ D. Bisello,⁴³ I. Bizjak,³¹ R. E. Blair,² C. Blocker,⁶ B. Blumenfeld,²⁵ A. Bocci,¹⁶ A. Bodek,⁴⁹ V. Boisvert,⁴⁹ G. Bolla,⁴⁸ A. Bolshov,³³ D. Bortoletto,⁴⁸ J. Boudreau,⁴⁷ A. Boveia,¹⁰ B. Brau,¹⁰ L. Brigliadori,⁵ C. Bromberg,³⁶ E. Brubaker,¹³ J. Budagov,¹⁵ H. S. Budd,⁴⁹ S. Budd,²⁴ K. Burkett,¹⁷ G. Busetto,⁴³ P. Bussey,²¹ A. Buzatu,³⁴ K. L. Byrum,² S. Cabrera,^{16,q} M. Campanelli,²⁰ M. Campbell,³⁵ F. Canelli,¹⁷ A. Canepa,⁴⁵ S. Carillo,^{18,i} D. Carlsmith,⁵⁹ R. Carosi,⁴⁶ S. Carron,³⁴ B. Casal,¹¹ M. Casarsa,⁵⁴ A. Castro,⁵ P. Catastini,⁴⁶ D. Cauz,⁵⁴ M. Cavalli-Sforza,³ A. Cerri,²⁹ L. Cerrito,^{31,m} S. H. Chang,²⁸ Y. C. Chen,¹ M. Chertok,⁷ G. Chiarelli,⁴⁶ G. Chlachidze,¹⁷ F. Chlebana,¹⁷ I. Cho,²⁸ K. Cho,²⁸ D. Chokheli,¹⁵ J. P. Chou,²² G. Choudalakis,³³ S. H. Chuang,⁵² K. Chung,¹² W. H. Chung,⁵⁹ Y. S. Chung,⁴⁹ M. Cijlijak,⁴⁶ C. I. Ciobanu,²⁴ M. A. Ciocci,⁴⁶ A. Clark,²⁰ D. Clark,⁶ M. Coca,¹⁶ G. Compostella,⁴³ M. E. Convery,⁵⁰ J. Conway,⁷ B. Cooper,³¹ K. Copic,³⁵ M. Cordelli,¹⁹ G. Cortiana,⁴³ F. Crescioli,⁴⁶ C. Cuenca Almenar,^{7,q} J. Cuevas,^{11,l} R. Culbertson,¹⁷ J. C. Cully,³⁵ S. DaRonco,⁴³ M. Datta,¹⁷ S. D'Auria,²¹ T. Davies,²¹ D. Dagenhart,¹⁷ P. de Barbaro,⁴⁹ S. De Cecco,⁵¹ A. Deisher,²⁹ G. De Lentdecker,^{49,c} G. De Lorenzo,³ M. Dell'Orso,⁴⁶ F. Delli Paoli,⁴³ L. Demortier,⁵⁰ J. Deng,¹⁶ M. Deninno,⁵ D. De Pedis,⁵¹ P. F. Derwent,¹⁷ G. P. Di Giovanni,⁴⁴ C. Dionisi,⁵¹ B. Di Ruzza,⁵⁴ J. R. Dittmann,⁴ M. D'Onofrio,³ C. Dörr,²⁶ S. Donati,⁴⁶ P. Dong,⁸ J. Donini,⁴³ T. Dorigo,⁴³ S. Dube,⁵² J. Efron,³⁹ R. Erbacher,⁷ D. Errede,²⁴ S. Errede,²⁴ R. Eusebi,¹⁷ H. C. Fang,²⁹ S. Farrington,³⁰ I. Fedorko,⁴⁶ W. T. Fedorko,¹³ R. G. Feild,⁶⁰ M. Feindt,²⁶ J. P. Fernandez,³² R. Field,¹⁸ G. Flanagan,⁴⁸ R. Forrest,⁷ S. Forrester,⁷ M. Franklin,²² J. C. Freeman,²⁹ I. Furic,¹³ M. Gallinaro,⁵⁰ J. Galyardt,¹² J. E. Garcia,⁴⁶ F. Garberon,¹⁰ A. F. Garfinkel,⁴⁸ C. Gay,⁶⁰ H. Gerberich,²⁴ D. Gerdes,³⁵ S. Giagu,⁵¹ P. Giannetti,⁴⁶ K. Gibson,⁴⁷ J. L. Gimmell,⁴⁹ C. Ginsburg,¹⁷ N. Giokaris,^{15,a} M. Giordani,⁵⁴ P. Giromini,¹⁹ M. Giunta,⁴⁶ G. Giurgiu,²⁵ V. Glagolev,¹⁵ D. Glenzinski,¹⁷ M. Gold,³⁷ N. Goldschmidt,¹⁸ J. Goldstein,^{42,b} A. Golossanov,¹⁷ G. Gomez,¹¹ G. Gomez-Ceballos,³³ M. Goncharov,⁵³ O. González,³² I. Gorelov,³⁷ A. T. Goshaw,¹⁶ K. Goulios,⁵⁰ A. Gresele,⁴³ S. Grinstein,²² C. Grosso-Pilcher,¹³ R. C. Group,¹⁷ U. Grundler,²⁴ J. Guimaraes da Costa,²² Z. Gunay-Unalan,³⁶ C. Haber,²⁹ K. Hahn,³³ S. R. Hahn,¹⁷ E. Halkiadakis,⁵² A. Hamilton,²⁰ B.-Y. Han,⁴⁹ J. Y. Han,⁴⁹ R. Handler,⁵⁹ F. Happacher,¹⁹ K. Hara,⁵⁵ D. Hare,⁵² M. Hare,⁵⁶ S. Harper,⁴² R. F. Harr,⁵⁸ R. M. Harris,¹⁷ M. Hartz,⁴⁷ K. Hatakeyama,⁵⁰ J. Hauser,⁸ C. Hays,⁴² M. Heck,²⁶ A. Heijboer,⁴⁵ B. Heinemann,²⁹ J. Heinrich,⁴⁵ C. Henderson,³³ M. Herndon,⁵⁹ J. Heuser,²⁶ D. Hidas,¹⁶ C. S. Hill,^{10,b} D. Hirschbuehl,²⁶ A. Hocker,¹⁷ A. Holloway,²² S. Hou,¹ M. Houlden,³⁰ S.-C. Hsu,⁹ B. T. Huffman,⁴² R. E. Hughes,³⁹ U. Husemann,⁶⁰ J. Huston,³⁶ J. Incandela,¹⁰ G. Introzzi,⁴⁶ M. Iori,⁵¹ A. Ivanov,⁷ B. Iyutin,³³ E. James,¹⁷ D. Jang,⁵² B. Jayatilaka,¹⁶ D. Jeans,⁵¹ E. J. Jeon,²⁸ S. Jindariani,¹⁸ W. Johnson,⁷ M. Jones,⁴⁸ K. K. Joo,²⁸ S. Y. Jun,¹² J. E. Jung,²⁸ T. R. Junk,²⁴ T. Kamon,⁵³ P. E. Karchin,⁵⁸ Y. Kato,⁴¹ Y. Kemp,²⁶ R. Kephart,¹⁷ U. Kerzel,²⁶ V. Khotilovich,⁵³ B. Kilminster,³⁹ D. H. Kim,²⁸ H. S. Kim,²⁸ J. E. Kim,²⁸ M. J. Kim,¹⁷ S. B. Kim,²⁸ S. H. Kim,⁵⁵ Y. K. Kim,¹³ N. Kimura,⁵⁵ L. Kirsch,⁶ S. Klimentenko,¹⁸ M. Klute,³³ B. Knuteson,³³ B. R. Ko,¹⁶ K. Kondo,⁵⁷ D. J. Kong,²⁸ J. Konigsberg,¹⁸ A. Korytov,¹⁸ A. V. Kotwal,¹⁶ A. C. Kraan,⁴⁵ J. Kraus,²⁴ M. Kreps,²⁶ J. Kroll,⁴⁵ N. Krumnack,⁴ M. Kruse,¹⁶ V. Krutelyov,¹⁰ T. Kubo,⁵⁵ S. E. Kuhlmann,² T. Kuhr,²⁶ N. P. Kulkarni,⁵⁸ Y. Kusakabe,⁵⁷ S. Kwang,¹³ A. T. Laasanen,⁴⁸ S. Lai,³⁴ S. Lami,⁴⁶ S. Lammel,¹⁷ M. Lancaster,³¹ R. L. Lander,⁷ K. Lannon,³⁹ A. Lath,⁵² G. Latino,⁴⁶ I. Lazzizzera,⁴³ T. LeCompte,² J. Lee,⁴⁹ J. Lee,²⁸ Y. J. Lee,²⁸ S. W. Lee,^{53,o} R. Lefèvre,²⁰ N. Leonardo,³³ S. Leone,⁴⁶ S. Levy,¹³ J. D. Lewis,¹⁷ C. Lin,⁶⁰ C. S. Lin,¹⁷ M. Lindgren,¹⁷ E. Lipeles,⁹ A. Lister,⁷ D. O. Litvintsev,¹⁷ T. Liu,¹⁷ N. S. Lockyer,⁴⁵ A. Loginov,⁶⁰ M. Loreti,⁴³ R.-S. Lu,¹ D. Lucchesi,⁴³ P. Lujan,²⁹ P. Lukens,¹⁷ G. Lungu,¹⁸ L. Lyons,⁴² J. Lys,²⁹ R. Lysak,¹⁴ E. Lytken,⁴⁸ P. Mack,²⁶ D. MacQueen,³⁴ R. Madrak,¹⁷ K. Maeshima,¹⁷ K. Makhoul,³³ T. Maki,²³ P. Maksimovic,²⁵ S. Malde,⁴² S. Malik,³¹ G. Manca,³⁰ F. Margaroli,⁵ R. Marginean,¹⁷ C. Marino,²⁶ C. P. Marino,²⁴ A. Martin,⁶⁰ M. Martin,²⁵ V. Martin,^{21,g} M. Martínez,³ R. Martínez-Ballarín,³² T. Maruyama,⁵⁵ P. Mastrandrea,⁵¹ T. Masubuchi,⁵⁵ H. Matsunaga,⁵⁵ M. E. Mattson,⁵⁸ R. Mazini,³⁴ P. Mazzanti,⁵ K. S. McFarland,⁴⁹ P. McIntyre,⁵³ R. McNulty,^{30,f} A. Mehta,³⁰ P. Mehtala,²³ S. Menzemer,^{11,h} A. Menzione,⁴⁶ P. Merkel,⁴⁸ C. Mesropian,⁵⁰ A. Messina,³⁶ T. Miao,¹⁷ N. Miladinovic,⁶ J. Miles,³³ R. Miller,³⁶ C. Mills,¹⁰ M. Milnik,²⁶ A. Mitra,¹ G. Mitselmakher,¹⁸ A. Miyamoto,²⁷ S. Moed,²⁰ N. Moggi,⁵ B. Mohr,⁸ C. S. Moon,²⁸ R. Moore,¹⁷ M. Morello,⁴⁶ P. Movilla Fernandez,²⁹ J. Mülmenstädt,²⁹ A. Mukherjee,¹⁷ Th. Muller,²⁶

R. Mumford,²⁵ P. Murat,¹⁷ M. Mussini,⁵ J. Nachtman,¹⁷ A. Nagano,⁵⁵ J. Naganoma,⁵⁷ K. Nakamura,⁵⁵ I. Nakano,⁴⁰ A. Napier,⁵⁶ V. Necula,¹⁶ C. Neu,⁴⁵ M. S. Neubauer,⁹ J. Nielsen,^{29,n} L. Nodulman,² O. Normiella,³ E. Nurse,³¹ S. H. Oh,¹⁶ Y. D. Oh,²⁸ I. Oksuzian,¹⁸ T. Okusawa,⁴¹ R. Oldeman,³⁰ R. Orava,²³ K. Osterberg,²³ C. Pagliarone,⁴⁶ E. Palencia,¹¹ V. Papadimitriou,¹⁷ A. Papaikonomou,²⁶ A. A. Paramonov,¹³ B. Parks,³⁹ S. Pashapour,³⁴ J. Patrick,¹⁷ G. Pauletta,⁵⁴ M. Paulini,¹² C. Paus,³³ D. E. Pellett,⁷ A. Penzo,⁵⁴ T. J. Phillips,¹⁶ G. Piacentino,⁴⁶ J. Piedra,⁴⁴ L. Pinera,¹⁸ K. Pitts,²⁴ C. Plager,⁸ L. Pondrom,⁵⁹ X. Portell,³ O. Poukhov,¹⁵ N. Pounder,⁴² F. Prakoshyn,¹⁵ A. Pronko,¹⁷ J. Proudfoot,² F. Ptohos,^{19,e} G. Punzi,⁴⁶ J. Pursley,²⁵ J. Rademacker,^{42,b} A. Rahaman,⁴⁷ V. Ramakrishnan,⁵⁹ N. Ranjan,⁴⁸ I. Redondo,³² B. Reisert,¹⁷ V. Rekovic,³⁷ P. Renton,⁴² M. Rescigno,⁵¹ S. Richter,²⁶ F. Rimondi,⁵ L. Ristori,⁴⁶ A. Robson,²¹ T. Rodrigo,¹¹ E. Rogers,²⁴ S. Rolli,⁵⁶ R. Roser,¹⁷ M. Rossi,⁵⁴ R. Rossin,¹⁰ P. Roy,³⁴ A. Ruiz,¹¹ J. Russ,¹² V. Rusu,¹³ H. Saarikko,²³ A. Safonov,⁵³ W. K. Sakumoto,⁴⁹ G. Salamanna,⁵¹ O. Saltó,³ L. Santi,⁵⁴ S. Sarkar,⁵¹ L. Sartori,⁴⁶ K. Sato,¹⁷ P. Savard,³⁴ A. Savoy-Navarro,⁴⁴ T. Scheidle,²⁶ P. Schlabach,¹⁷ E. E. Schmidt,¹⁷ M. P. Schmidt,⁶⁰ M. Schmitt,³⁸ T. Schwarz,⁷ L. Scodellaro,¹¹ A. L. Scott,¹⁰ A. Scribano,⁴⁶ F. Scuri,⁴⁶ A. Sedov,⁴⁸ S. Seidel,³⁷ Y. Seiya,⁴¹ A. Semenov,¹⁵ L. Sexton-Kennedy,¹⁷ A. Sfyrla,²⁰ S. Z. Shalhout,⁵⁸ M. D. Shapiro,²⁹ T. Shears,³⁰ P. F. Shepard,⁴⁷ D. Sherman,²² M. Shimojima,^{55,k} M. Shochet,¹³ Y. Shon,⁵⁹ I. Shreyber,²⁰ A. Sidoti,⁴⁶ P. Sinervo,³⁴ A. Sisakyan,¹⁵ A. J. Slaughter,¹⁷ J. Slaunwhite,³⁹ K. Sliwa,⁵⁶ J. R. Smith,⁷ F. D. Snider,¹⁷ R. Snihur,³⁴ M. Soderberg,³⁵ A. Soha,⁷ S. Somalwar,⁵² V. Sorin,³⁶ J. Spalding,¹⁷ F. Spinella,⁴⁶ T. Spreitzer,³⁴ P. Squillacioti,⁴⁶ M. Stanitzki,⁶⁰ A. Staveris-Polykalas,⁴⁶ R. St. Denis,²¹ B. Stelzer,⁸ O. Stelzer-Chilton,⁴² D. Stentz,³⁸ J. Strologas,³⁷ D. Stuart,¹⁰ J. S. Suh,²⁸ A. Sukhanov,¹⁸ H. Sun,⁵⁶ I. Suslov,¹⁵ T. Suzuki,⁵⁵ A. Taffard,^{24,p} R. Takashima,⁴⁰ Y. Takeuchi,⁵⁵ R. Tanaka,⁴⁰ M. Tecchio,³⁵ P. K. Teng,¹ K. Terashi,⁵⁰ J. Thom,^{17,d} A. S. Thompson,²¹ E. Thomson,⁴⁵ P. Tipton,⁶⁰ V. Tiwari,¹² S. Tkaczyk,¹⁷ D. Toback,⁵³ S. Tokar,¹⁴ K. Tollefson,³⁶ T. Tomura,⁵⁵ D. Tonelli,⁴⁶ S. Torre,¹⁹ D. Torretta,¹⁷ S. Tourneur,⁴⁴ W. Trischuk,³⁴ R. Tsuchiya,⁵⁷ S. Tsuno,⁴⁰ Y. Tu,⁴⁵ N. Turini,⁴⁶ F. Ukegawa,⁵⁵ S. Uozumi,⁵⁵ S. Vallecorsa,²⁰ N. van Remortel,²³ A. Varganov,³⁵ E. Vataga,³⁷ F. Vázquez,^{18,i} G. Velez,¹⁷ G. Veramendi,²⁴ V. Veszpremi,⁴⁸ M. Vidal,³² R. Vidal,¹⁷ I. Vila,¹¹ R. Vilar,¹¹ T. Vine,³¹ I. Vollrath,³⁴ I. Volobouev,^{29,o} G. Volpi,⁴⁶ F. Würthwein,⁹ P. Wagner,⁵³ R. G. Wagner,² R. L. Wagner,¹⁷ J. Wagner,²⁶ W. Wagner,²⁶ R. Wallny,⁸ S. M. Wang,¹ A. Warburton,³⁴ D. Waters,³¹ M. Weinberger,⁵³ W. C. Wester III,¹⁷ B. Whitehouse,⁵⁶ D. Whiteson,⁴⁵ A. B. Wicklund,² E. Wicklund,¹⁷ G. Williams,³⁴ H. H. Williams,⁴⁵ P. Wilson,¹⁷ B. L. Winer,³⁹ P. Wittich,^{17,d} S. Wolbers,¹⁷ C. Wolfe,¹³ T. Wright,³⁵ X. Wu,²⁰ S. M. Wynne,³⁰ A. Yagil,⁹ K. Yamamoto,⁴¹ J. Yamaoka,⁵² T. Yamashita,⁴⁰ C. Yang,⁶⁰ U. K. Yang,^{13,j} Y. C. Yang,²⁸ W. M. Yao,²⁹ G. P. Yeh,¹⁷ J. Yoh,¹⁷ K. Yorita,¹³ T. Yoshida,⁴¹ G. B. Yu,⁴⁹ I. Yu,²⁸ S. S. Yu,¹⁷ J. C. Yun,¹⁷ L. Zanello,⁵¹ A. Zanetti,⁵⁴ I. Zaw,²² X. Zhang,²⁴ J. Zhou,⁵² and S. Zucchelli⁵

(CDF Collaboration)

¹*Institute of Physics, Academia Sinica, Taipei, Taiwan 11529, Republic of China*²*Argonne National Laboratory, Argonne, Illinois 60439, USA*³*Institut de Física d'Altes Energies, Universitat Autònoma de Barcelona, E-08193, Bellaterra (Barcelona), Spain*⁴*Baylor University, Waco, Texas 76798, USA*⁵*Istituto Nazionale di Fisica Nucleare, University of Bologna, I-40127 Bologna, Italy*⁶*Brandeis University, Waltham, Massachusetts 02254, USA*⁷*University of California, Davis, Davis, California 95616, USA*⁸*University of California, Los Angeles, Los Angeles, California 90024, USA*⁹*University of California, San Diego, La Jolla, California 92093, USA*¹⁰*University of California, Santa Barbara, Santa Barbara, California 93106, USA*¹¹*Instituto de Física de Cantabria, CSIC-University of Cantabria, 39005 Santander, Spain*¹²*Carnegie Mellon University, Pittsburgh, Pennsylvania 15213, USA*¹³*Enrico Fermi Institute, University of Chicago, Chicago, Illinois 60637, USA*¹⁴*Comenius University, 842 48 Bratislava, Slovakia,**and Institute of Experimental Physics, 040 01 Kosice, Slovakia*¹⁵*Joint Institute for Nuclear Research, RU-141980 Dubna, Russia*¹⁶*Duke University, Durham, North Carolina 27708, USA*¹⁷*Fermi National Accelerator Laboratory, Batavia, Illinois 60510, USA*¹⁸*University of Florida, Gainesville, Florida 32611, USA*¹⁹*Laboratori Nazionali di Frascati, Istituto Nazionale di Fisica Nucleare, I-00044 Frascati, Italy*²⁰*University of Geneva, CH-1211 Geneva 4, Switzerland*²¹*Glasgow University, Glasgow G12 8QQ, United Kingdom*²²*Harvard University, Cambridge, Massachusetts 02138, USA*

- ²³*Division of High Energy Physics, Department of Physics, University of Helsinki and Helsinki Institute of Physics, FIN-00014, Helsinki, Finland*
- ²⁴*University of Illinois, Urbana, Illinois 61801, USA*
- ²⁵*The Johns Hopkins University, Baltimore, Maryland 21218, USA*
- ²⁶*Institut für Experimentelle Kernphysik, Universität Karlsruhe, 76128 Karlsruhe, Germany*
- ²⁷*High Energy Accelerator Research Organization (KEK), Tsukuba, Ibaraki 305, Japan*
- ²⁸*Center for High Energy Physics: Kyungpook National University, Taegu 702-701, Korea; Seoul National University, Seoul 151-742, Korea; SungKyunKwan University, Suwon 440-746, Korea*
- ²⁹*Ernest Orlando Lawrence Berkeley National Laboratory, Berkeley, California 94720, USA*
- ³⁰*University of Liverpool, Liverpool L69 7ZE, United Kingdom*
- ³¹*University College London, London WC1E 6BT, United Kingdom*
- ³²*Centro de Investigaciones Energeticas Medioambientales y Tecnologicas, E-28040 Madrid, Spain*
- ³³*Massachusetts Institute of Technology, Cambridge, Massachusetts 02139, USA*
- ³⁴*Institute of Particle Physics: McGill University, Montréal, Canada H3A 2T8; and University of Toronto, Toronto, Canada M5S 1A7*
- ³⁵*University of Michigan, Ann Arbor, Michigan 48109, USA*
- ³⁶*Michigan State University, East Lansing, Michigan 48824, USA*
- ³⁷*University of New Mexico, Albuquerque, New Mexico 87131, USA*
- ³⁸*Northwestern University, Evanston, Illinois 60208, USA*
- ³⁹*The Ohio State University, Columbus, Ohio 43210, USA*
- ⁴⁰*Okayama University, Okayama 700-8530, Japan*
- ⁴¹*Osaka City University, Osaka 588, Japan*
- ⁴²*University of Oxford, Oxford OX1 3RH, United Kingdom*
- ⁴³*University of Padova, Istituto Nazionale di Fisica Nucleare, Sezione di Padova-Trento, I-35131 Padova, Italy*
- ⁴⁴*LPNHE, Universite Pierre et Marie Curie/IN2P3-CNRS, UMR7585, Paris, F-75252 France*
- ⁴⁵*University of Pennsylvania, Philadelphia, Pennsylvania 19104, USA*
- ⁴⁶*Istituto Nazionale di Fisica Nucleare Pisa, Universities of Pisa, Siena and Scuola Normale Superiore, I-56127 Pisa, Italy*
- ⁴⁷*University of Pittsburgh, Pittsburgh, Pennsylvania 15260, USA*
- ⁴⁸*Purdue University, West Lafayette, Indiana 47907, USA*
- ⁴⁹*University of Rochester, Rochester, New York 14627, USA*
- ⁵⁰*The Rockefeller University, New York, New York 10021, USA*
- ⁵¹*Istituto Nazionale di Fisica Nucleare, Sezione di Roma 1, University of Rome "La Sapienza," I-00185 Roma, Italy*
- ⁵²*Rutgers University, Piscataway, New Jersey 08855, USA*
- ⁵³*Texas A&M University, College Station, Texas 77843, USA*
- ⁵⁴*Istituto Nazionale di Fisica Nucleare, University of Trieste/Udine, Italy*
- ⁵⁵*University of Tsukuba, Tsukuba, Ibaraki 305, Japan*
- ⁵⁶*Tufts University, Medford, Massachusetts 02155, USA*
- ⁵⁷*Waseda University, Tokyo 169, Japan*
- ⁵⁸*Wayne State University, Detroit, Michigan 48201, USA*
- ⁵⁹*University of Wisconsin, Madison, Wisconsin 53706, USA*
- ⁶⁰*Yale University, New Haven, Connecticut 06520, USA*
- (Received 3 April 2007; published 26 September 2007)

We have measured the polarizations of J/ψ and $\psi(2S)$ mesons as functions of their transverse momentum p_T when they are produced promptly in the rapidity range $|y| < 0.6$ with $p_T \geq 5$ GeV/ c . The analysis is performed using a data sample with an integrated luminosity of about 800 pb⁻¹ collected by the CDF II detector. For both vector mesons, we find that the polarizations become increasingly longitudinal as p_T increases from 5 to 30 GeV/ c . These results are compared to the predictions of nonrelativistic quantum chromodynamics and other contemporary models. The effective polarizations of J/ψ and $\psi(2S)$ mesons from B -hadron decays are also reported.

DOI: [10.1103/PhysRevLett.99.132001](https://doi.org/10.1103/PhysRevLett.99.132001)

PACS numbers: 13.88.+e, 13.20.Gd, 14.40.Lb

An effective field theory, nonrelativistic quantum chromodynamics (NRQCD) [1], provides a rigorous formalism for calculating the production rates of charmonium ($c\bar{c}$) states. NRQCD explains the direct production cross sections for J/ψ and $\psi(2S)$ mesons observed at the Tevatron [2,3] and predicts their increasingly transverse polariza-

tions as p_T increases, where p_T is the meson's momentum component perpendicular to the colliding beam direction [4]. The first polarization measurements at the Tevatron [5] did not show such a trend. This Letter reports on J/ψ and $\psi(2S)$ polarization measurements with a larger data sample than previously available. This allows the extension of the

measurement to a higher p_T region and makes a more stringent test of the NRQCD prediction.

The NRQCD cross section calculation for $c\bar{c}$ production separates the long-distance nonperturbative contributions from the short-distance perturbative behavior. The former is treated as an expansion of the matrix elements in powers of the nonrelativistic charm-quark velocity. This expansion can be computed by lattice simulations, but currently the expansion coefficients are treated as universal parameters, which are adjusted to match the cross section measurements at the Tevatron [2,3]. The calculation also applies to $c\bar{c}$ production in ep collisions, but HERA measurements of J/ψ polarization tend to disagree with the NRQCD prediction [6]. These difficulties have led some authors to explore alternative power expansions of the long-distance interactions for the $c\bar{c}$ system [7]. There are also new QCD-inspired models, the gluon tower model [8] and the k_T -factorization model [9], that accommodate vector-meson cross sections at both HERA and the Tevatron and predict the vector-meson polarizations as functions of p_T . These authors emphasize that measuring the vector-meson polarizations as functions of p_T is a crucial test of NRQCD.

The CDF II detector is described in detail elsewhere [3,10]. In this analysis, the essential features are a muon system covering the central region of pseudorapidity, $|\eta| < 0.6$, and the tracking system, immersed in the 1.4 T solenoidal magnetic field and composed of a silicon microstrip detector and a cylindrical drift chamber called the central outer tracker (COT). The data used here correspond to an integrated luminosity of about 800 pb^{-1} and were recorded between June 2004 and February 2006 by a dimuon trigger, which requires two opposite-charge muon candidates, each having $p_T > 1.5 \text{ GeV}/c$.

Decays of vector mesons V [either J/ψ or $\psi(2S)$] $\rightarrow \mu^+ \mu^-$ are selected from dimuon events for which each

track has segments reconstructed in both the COT and the silicon microstrip detector. The p_T of each muon is required to exceed $1.75 \text{ GeV}/c$ in order to guarantee a well-measured trigger efficiency. The muon track pair is required to be consistent with originating from a common vertex and to have an invariant mass M within the range $2.8(3.4) < M < 3.4(3.9) \text{ GeV}/c^2$ to be considered as a J/ψ [$\psi(2S)$] candidate. To have a reasonable polarization sensitivity, the vector-meson candidates are required to have $p_T \geq 5 \text{ GeV}/c$ in the rapidity range $|y| \equiv \frac{1}{2} \ln[(E + p_{\parallel})/(E - p_{\parallel})] < 0.6$, where E is the energy and p_{\parallel} is the momentum parallel to the beam direction of the dimuon system. Events are separated into a signal region and sideband regions, as indicated in Fig. 1. The fit to the data uses a double (single) Gaussian for the J/ψ [$\psi(2S)$] signal and a linear background shape. The fits are used only to define signal and background regions. The signal regions are within $3\sigma_V$ of the fitted mass peaks M_V , where σ_V is the width obtained in the fit to the invariant mass distribution. Both the background distribution and the quantity of background events under the signal peak are estimated by events from the lower and upper mass sidebands. The sideband regions are $7\sigma_{J/\psi}$ ($4\sigma_{\psi(2S)}$) away from the signal region for J/ψ [$\psi(2S)$].

For each candidate, we compute $ct = ML_{xy}/p_T$, where t is the proper decay time and L_{xy} is the transverse distance between the beam line and the decay vertex in the plane normal to the beam direction. The ct distributions of the selected dimuon events are shown in Fig. 2. The ct distribution of prompt events is a Gaussian distribution centered at zero due to finite tracking resolution. For J/ψ , the prompt events are due to direct production or the decays of heavier charmonium states such as χ_c and $\psi(2S)$; for $\psi(2S)$, the prompt events are almost entirely due to direct production since heavier charmonium states rarely decay

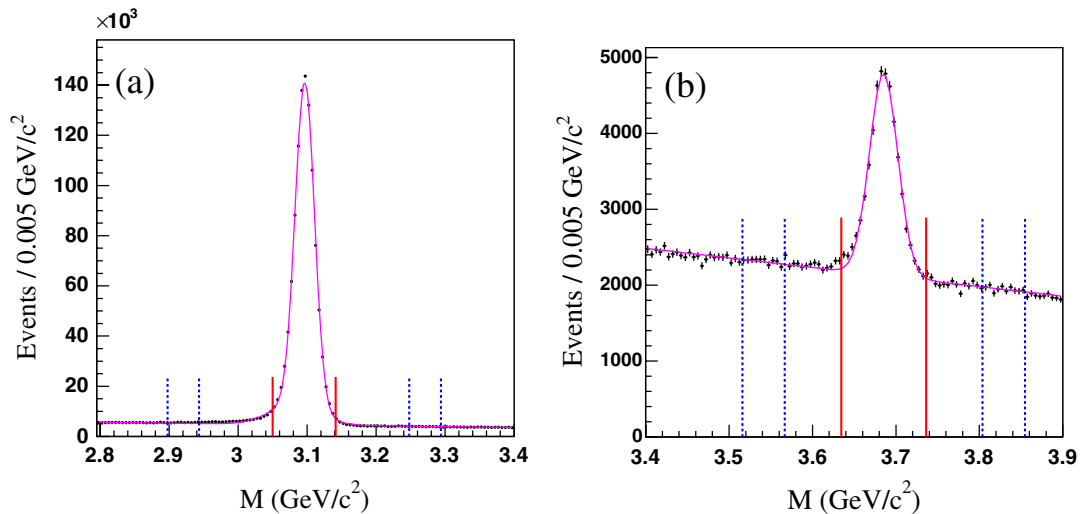


FIG. 1 (color online). Invariant mass distributions for (a) J/ψ and (b) $\psi(2S)$ candidates. The curves are fits to the data. The solid (dashed) lines indicate the signal (sideband) regions.

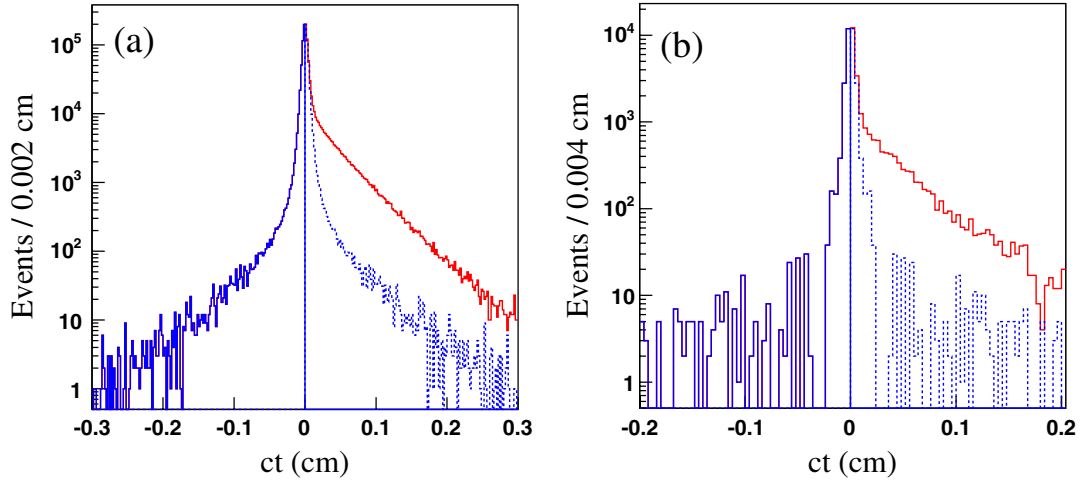


FIG. 2 (color online). Sideband-subtracted ct distributions for (a) J/ψ and (b) $\psi(2S)$ events. The prompt Gaussian peak, positive excess from B -hadron decays, and negative tail from mismeasured events are shown. The dotted line is the reflection of the negative ct histogram about zero.

to $\psi(2S)$ [11]. Both the J/ψ and the $\psi(2S)$ samples contain significant numbers of events originating from long-lived B -hadron decays, as can be seen from the event excess at positive ct . We have measured the fraction of $B \rightarrow J/\psi + X$ events in the J/ψ sample and found agreement with other results [3]. We select prompt events by requiring the sum of the squared impact parameter significances of the positively and negatively charged muon tracks $S \equiv (d_0^+/\sigma^+)^2 + (d_0^-/\sigma^-)^2 \leq 8$. The impact parameter d_0 is the distance of closest approach of the track to the beam line in the transverse plane. Vector-meson candidates from B -hadron decays are selected by requiring $S > 16$ and $ct > 0.03$ cm. This requirement retains a negligible fraction of prompt events in the B sample.

To measure the polarizations of prompt J/ψ and $\psi(2S)$ mesons as functions of p_T , the J/ψ events are analyzed in six p_T bins and the $\psi(2S)$ events in three bins, shown in Table I. We determine the fraction of B -decay background remaining in prompt samples f_{bkd} by subtracting the number of negative ct events from the number of positive ct events. Only a negligible fraction ($<0.2\%$) of B decays

produce vector-meson events with negative ct . For both vector mesons, f_{bkd} increases with p_T , as listed in Table I. The prompt polarization from the fitting algorithm is corrected for this contamination.

The polarization information is contained in the distribution of the muon decay angle θ^* , the angle of the μ^+ in the rest frame of the vector meson with respect to the vector-meson boost direction in the laboratory system. The decay angle distribution depends on the polarization parameter α : $dN/d\cos\theta^* \propto 1 + \alpha\cos^2\theta^*$ ($-1 \leq \alpha \leq 1$). For fully transverse (longitudinal) polarization, $\alpha = +1$ (-1). Intermediate values of α indicate a mixture of transverse and longitudinal polarization.

A template method is used to account for acceptance and efficiency. Two sets of $\cos\theta^*$ distributions for fully polarized decays of J/ψ and $\psi(2S)$ events, one longitudinal (L) and the other transverse (T), are produced with the CDF simulation program using the efficiency-corrected p_T spectra measured from data [3,12]. We use the muon trigger efficiency measured using data as a function of track parameters (p_T , η , ϕ) to account for detector non-

TABLE I. Polarization parameter α for prompt production in each p_T bin. The first (second) uncertainty is statistical (systematic). $\langle p_T \rangle$ is the average transverse momentum.

	p_T (GeV/ c)	$\langle p_T \rangle$ (GeV/ c)	f_{bkd} (%)	α	$\chi^2/\text{d.o.f}$
J/ψ	5–6	5.5	2.8 ± 0.2	$-0.004 \pm 0.029 \pm 0.009$	15.5/21
	6–7	6.5	3.4 ± 0.2	$-0.015 \pm 0.028 \pm 0.010$	24.1/23
	7–9	7.8	4.1 ± 0.2	$-0.077 \pm 0.023 \pm 0.013$	35.1/25
	9–12	10.1	5.7 ± 0.3	$-0.094 \pm 0.028 \pm 0.007$	34.0/29
	12–17	13.7	6.7 ± 0.6	$-0.140 \pm 0.043 \pm 0.007$	35.0/31
	17–30	20.0	13.6 ± 1.4	$-0.187 \pm 0.090 \pm 0.007$	33.9/35
$\psi(2S)$	5–7	5.9	1.6 ± 0.9	$+0.314 \pm 0.242 \pm 0.028$	13.1/11
	7–10	8.2	4.9 ± 1.2	$-0.013 \pm 0.201 \pm 0.035$	18.5/13
	10–30	12.6	8.6 ± 1.8	$-0.374 \pm 0.222 \pm 0.062$	26.9/17

uniformities. The parametrized efficiency is used as a filter on all simulated muons. Events that pass reconstruction represent the behavior of fully polarized vector-meson decays in the detector.

The fitting algorithm [5] uses two binned $\cos\theta^*$ distributions for each p_T bin, one made by N_S events from the signal region (signal plus background) and the other made by N_B events from the sideband regions (background). The χ^2 minimization is done simultaneously for both $\cos\theta^*$ distributions. The fitting algorithm includes an individual background term for each $\cos\theta^*$ bin, normalized to N_B . Simulation shows that the $\cos\theta^*$ resolution at all decay angles over the entire p_T range is much smaller than the bin width of 0.05 [0.10 for $\psi(2S)$] used here. The data, fit, and template distributions for the worst fit (9% probability) in the J/ψ data are shown in Fig. 3.

All systematic uncertainties are much smaller than the statistical uncertainties. Varying the p_T spectrum used in the simulation by 1σ changed the polarization parameter for J/ψ at most by 0.002. A systematic uncertainty of 0.007 was estimated by the change in the polarization parameter when a modification was made on all trigger efficiencies by $\pm 1\sigma$. For $\psi(2S)$, the dominant systematic uncertainty came from the yield estimate because of the radiative tail and the large background. The total systematic uncertainties shown in Table I were taken to be the quadrature sum of these individual uncertainties. Other possible sources of systematic uncertainties—signal definition and $\cos\theta^*$ binning—were determined to be negligible. Corrections to prompt polarization from B -decay contamination were small, so that uncertainties on B -decay polarization measurements also had negligible effect. No ϕ dependence of the polarizations was observed.

The polarization of J/ψ mesons from inclusive B_u and B_d decays was measured by the BABAR Collaboration [13]. In this analysis, the B -hadron direction is unknown, so we define θ^* with respect to the J/ψ direction in the

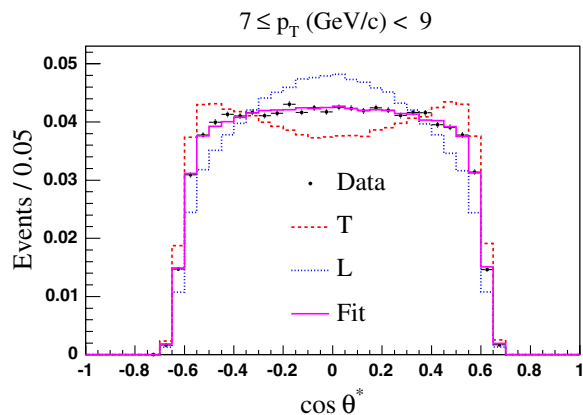


FIG. 3 (color online). $\cos\theta^*$ distribution of data (points) and polarization fit for the worst χ^2 probability bin in the J/ψ data. The dotted (dashed) line is the template for fully L (T) polarization. The fit describes the overall trend of the data well.

laboratory system. The resulting polarization is somewhat diluted. As discussed in Ref. [3], CDF uses a Monte Carlo procedure to adapt the BABAR measurement to predict the effective J/ψ polarization parameter. For the J/ψ events with $5 \leq p_T < 30$ GeV/ c , the CDF model for B_u and B_d decays gives $\alpha_{\text{eff}} = -0.145 \pm 0.009$, independent of p_T . We have measured the polarization of vector mesons from B -hadron decays. For J/ψ , we find $\alpha_{\text{eff}} = -0.106 \pm 0.033(\text{stat}) \pm 0.007(\text{syst})$. At this level of accuracy, a polarization contribution by J/ψ mesons from B_s and b -baryon decays cannot be separated from the effective polarization due to those from B_u and B_d decays. We also report the first measurement of the $\psi(2S)$ polarization from B -hadron decays: $\alpha_{\text{eff}} = 0.36 \pm 0.25(\text{stat}) \pm 0.03(\text{syst})$.

The polarization parameters for both prompt vector mesons corrected for f_{bkd} using our experimental results on α_{eff} are listed as functions of p_T in Table I and are plotted in Fig. 4. The polarization parameters for J/ψ are negative over the entire p_T range of measurement and become increasingly negative (favoring longitudinal polarization) as p_T increases. For $\psi(2S)$, the central value of the polarization parameter is positive at small p_T , but, given the uncertainties, its behavior is consistent with the trend shown in the measurement of the J/ψ polarization.

The polarization behavior measured previously with 110 pb^{-1} [5] is not consistent with the results presented here. This is a differential measurement, and the muon efficiencies in this analysis are true dimuon efficiencies. In Ref. [5], they are the product of independent single muon efficiencies. The efficiency for muons with $p_T < 4$ GeV/ c is crucial for good polarization sensitivity. In this analysis, the muon efficiency varies smoothly from 99% to 97% over this range. In the analysis of Ref. [5], it varied from 93% to 40% with significant jumps between individual data points. Data from periods of drift chamber aging were omitted from this analysis because the polarization results were inconsistent with the remainder of the data. Studies such as this were not done in the analysis of Ref. [5]. The systematics of the polarization measurement are much better understood in this analysis.

These polarization measurements for the charmed vector mesons extend to a p_T regime where perturbative QCD should be applicable. The results are compared to the predictions of NRQCD and the k_T -factorization model in Fig. 4. The prediction of the k_T -factorization model is presented for $p_T < 20$ GeV/ c and does not include the contribution from the decays of heavier charmonium states for J/ψ production. The polarizations for prompt production of both vector mesons become increasingly longitudinal as p_T increases beyond 10 GeV/ c . This behavior is in strong disagreement with the NRQCD prediction of large transverse polarization at high p_T . It is striking that the NRQCD calculation and the other models reproduce the measured J/ψ and $\psi(2S)$ cross sections at the Tevatron but fail to describe the polarization at high p_T . This indicates

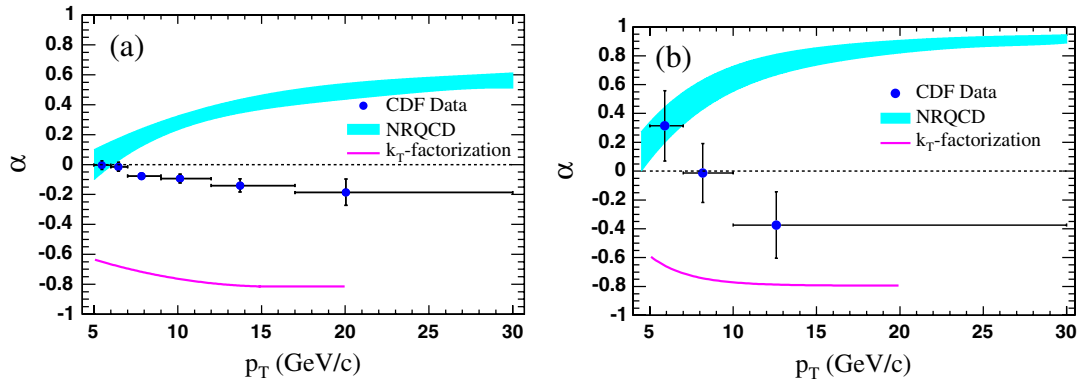


FIG. 4 (color online). Prompt polarizations as functions of p_T : (a) J/ψ and (b) $\psi(2S)$. The band (line) is the prediction from NRQCD [4] (the k_T -factorization model [9]).

that there is some important aspect of the production mechanism that is not yet understood.

We thank the Fermilab staff and the technical staffs of the participating institutions for their vital contributions. This work was supported by the U.S. Department of Energy and National Science Foundation; the Italian Istituto Nazionale di Fisica Nucleare; the Ministry of Education, Culture, Sports, Science and Technology of Japan; the Natural Sciences and Engineering Research Council of Canada; the National Science Council of the Republic of China; the Swiss National Science Foundation; the A.P. Sloan Foundation; the Bundesministerium für Bildung und Forschung, Germany; the Korean Science and Engineering Foundation and the Korean Research Foundation; the Particle Physics and Astronomy Research Council and the Royal Society, United Kingdom; the Institut National de Physique Nucleaire et Physique des Particules/CNRS; the Russian Foundation for Basic Research; the Comisión Interministerial de Ciencia y Tecnología, Spain; the European Community's Human Potential Programme; the Slovak R&D Agency; and the Academy of Finland.

^aVisiting scientist from University of Athens.

^bVisiting scientist from University of Bristol.

^cVisiting scientist from University Libre de Bruxelles.

^dVisiting scientist from Cornell University.

^eVisiting scientist from University of Cyprus.

^fVisiting scientist from University of Dublin.

^gVisiting scientist from University of Edinburgh.

^hVisiting scientist from University of Heidelberg.

ⁱVisiting scientist from Universidad Iberoamericana.

^jVisiting scientist from University of Manchester.

^kVisiting scientist from Nagasaki Institute of Applied Science.

^lVisiting scientist from University de Oviedo.

^mVisiting scientist from University of London, Queen Mary College.

ⁿVisiting scientist from University of California, Santa Cruz.

^oVisiting scientist from Texas Tech University.

^pVisiting scientist from University of California, Irvine.

^qVisiting scientist from IFIC(CSIC-Universitat de Valencia).

- [1] G. T. Bodwin, E. Braaten, and G. P. Lepage, Phys. Rev. D **51**, 1125 (1995); **55**, 5853 (1997); E. Braaten and S. Fleming, Phys. Rev. Lett. **74**, 3327 (1995).
- [2] F. Abe *et al.* (CDF Collaboration), Phys. Rev. Lett. **79**, 572 (1997).
- [3] D. Acosta *et al.* (CDF Collaboration), Phys. Rev. D **71**, 032001 (2005).
- [4] P. Cho and M. Wise, Phys. Lett. B **346**, 129 (1995); M. Beneke and I. Z. Rothstein, Phys. Lett. B **372**, 157 (1996); **389**, 769 (1996); E. Braaten, B. A. Kniehl, and J. Lee, Phys. Rev. D **62**, 094005 (2000).
- [5] T. Affolder *et al.* (CDF Collaboration), Phys. Rev. Lett. **85**, 2886 (2000).
- [6] C. Adloff *et al.* (H1 Collaboration), Eur. Phys. J. C **25**, 41 (2002); S. Chekanov *et al.* (ZEUS Collaboration), Eur. Phys. J. C **44**, 13 (2005).
- [7] S. Fleming, I. Z. Rothstein, and A. K. Leibovich, Phys. Rev. D **64**, 036002 (2001).
- [8] V. A. Khoze, A. D. Martin, M. G. Ryskin, and W. J. Stirling, Eur. Phys. J. C **39**, 163 (2005).
- [9] S. P. Baranov, Phys. Rev. D **66**, 114003 (2002).
- [10] The CDF coordinate system has \hat{z} along the proton direction, \hat{x} horizontal pointing outward from the Tevatron ring, and \hat{y} vertical. θ (ϕ) is the polar (azimuthal) angle measured with respect to \hat{z} , and η is the pseudorapidity defined as $-\ln[\tan(\theta/2)]$. The transverse momentum of a particle is denoted as $p_T = p \sin\theta$.
- [11] W.-M. Yao *et al.* (Particle Data Group), J. Phys. G **33**, 1 (2006).
- [12] A Letter on $\psi(2S)$ cross section measurement is in preparation.
- [13] B. Aubert *et al.* (BABAR Collaboration), Phys. Rev. D **67**, 032002 (2003).